Unconventional Pairing Originating from the Disconnected Fermi Surfaces of Superconducting $LaFeAsO_{1-x}F_x$

Kazuhiko Kuroki,[1] Seiichiro Onari,[2] Ryotaro Arita,[3,*] Hidetomo Usui,[1] Yukio Tanaka,[2] Hiroshi Kontani,[4] and Hideo Aoki[5]

[1]*Department of Applied Physics and Chemistry, The University of Electro -Communications, Chofu, Tokyo 182-8585, Japan*
[2]*Department of Applied Physics, Nagoya University, and CREST-JST, Nagoya 464-8603, Japan*
[3]*RIKEN, 2-1 Hirosawa, Wako, Saitama 351-0198, Japan*
[4]*Department of Physics, Nagoya University, Nagoya 464-8602, Japan*
[5]*Department of Physics, University of Tokyo, Tokyo 113-0033, Japan*

(Received 27 March 2008; published 22 August 2008)

For a newly discovered iron-based high T_c superconductor $LaFeAsO_{1-x}F_x$, we have constructed a minimal model, where inclusion of all five Fe d bands is found to be necessary. The random-phase approximation is applied to the model to investigate the origin of superconductivity. We conclude that the multiple spin-fluctuation modes arising from the nesting across the disconnected Fermi surfaces realize an extended s-wave pairing, while d-wave pairing can also be another candidate.

DOI: 10.1103/PhysRevLett.101.087004 PACS numbers: 74.20.−z, 74.25.Jb, 74.70.Dd

Understanding the mechanism of unconventional superconductivity (SC) has been one of the most challenging problems in condensed-matter physics. There is a renewed fascination with a recent discovery of SC in an iron-based superconductor $LaFeAsO_{1-x}F_x$ [1], which is likely to provide a fresh avenue for such a challenge. LaFeAsO belongs to the family of quaternary oxypnictides LnMPnO (Ln = La, Pr; M = Mn, Fe, Co, and Ni; Pn = P, As), which was originally fabricated by Zimmer *et al.* and Quebe *et al.* [2,3] For this family of compounds, Kamihara *et al.* first reported that LaFePO exhibits SC with $T_c \simeq 3$ K, which was raised to $T_c \simeq 7$ K by F doping [4]. SC has also been found in nickel-based compounds with the same structure [5]. Very recently, Kamihara *et al.* have come up with the discovery of SC in $LaFeAsO_{1-x}F_x$, where the F doping with $x \simeq 0.11$ leads to a remarkable $T_c \sim 26$ K.

The high value of T_c itself, confirmed also by Chen *et al.* [6], suggests the possibility of unconventional SC, but direct evidences is accumulating: A specific-heat measurement in magnetic fields shows that the coefficient γ displays $\sqrt{H}$ behavior [7]. A point-contact conductance measurement exhibits spectra with a distinct zero-bias peak [8], suggestive of the presence of sign change in the gap function [9–12]. The starting material, LaFeAsO, is a bad metal with some anomaly in the resistivity around 100 K [1]. As the system becomes metallic upon F doping, the uniform susceptibility exhibits Curie-Weiss behavior. Anomalies in the normal-state transport properties have also been reported for doped systems [13].

Theoretically, a first-principles band structure has been obtained for LaFePO [14], and more recently for LaFeAsO and related materials [15–18]. These band structures are metallic with five pieces (sheets) of the Fermi surface in the undoped system, which contradicts the experiment for undoped LaFeAsO [1]. However, a dynamical mean-field study shows that the electron correlation enhances the crystal field splitting, which leads to band-semiconducting behavior in accord with the experiment [16]. Local spin-density calculations for LaFeAsO show that the system is around the border between magnetic and nonmagnetic states, with a tendency toward ferromagnetism and antiferromagnetism [15,17]. It is also pointed out that the electron-phonon coupling is too weak to account for T_c = 26 K [7,18].

Given this background, the purpose of the present Letter is to first construct a microscopic electronic model for $LaFeAsO_{1-x}F_x$, which then serves as the basis for identifying the possible mechanisms for why this material favors high-T_c. The minimal model has turned out to contain all five Fe d orbitals, to which we have applied the random-phase approximation (RPA) to solve the Eliashberg equation. We shall conclude that a peculiar Fermi surface consisting of multiple pockets and ensuing multiple spin-fluctuation modes realize an unconventional s-wave pairing, while d-wave pairing can also be another candidate.

LaFeAsO has a tetragonal layered structure, in which Fe atoms are arrayed on a square lattice. Because of the tetrahedral coordination of As, there are two Fe atoms per unit cell. Each Fe layer is then sandwiched between LaO layers. The experimentally determined lattice constants are $a = 4.03552$ Å and $c = 8.7393$ Å, with two internal coordinates $z_{\mathrm{La}} = 0.1415$ and $z_{\mathrm{As}} = 0.6512$. We have obtained the band structure [Fig. 1(a), inset] with the Quantum-ESPRESSO package [19], and then construct the maximally localized Wannier functions [20]. These maximally localized Wannier functions, centered at the two Fe sites in the unit cell, have five orbital symmetries (orbital $1: d_{3Z^2-R^2}$, $2: d_{XZ}$, $3: d_{YZ}$, $4: d_{X^2-Y^2}$, $5: d_{XY}$, where X, Y, Z refer to those for the original unit cell). We can note that the two Wannier orbitals in each unit cell are equivalent in that each Fe atom has the same local arrangement of other atoms. We can thus take a unit cell that contains only

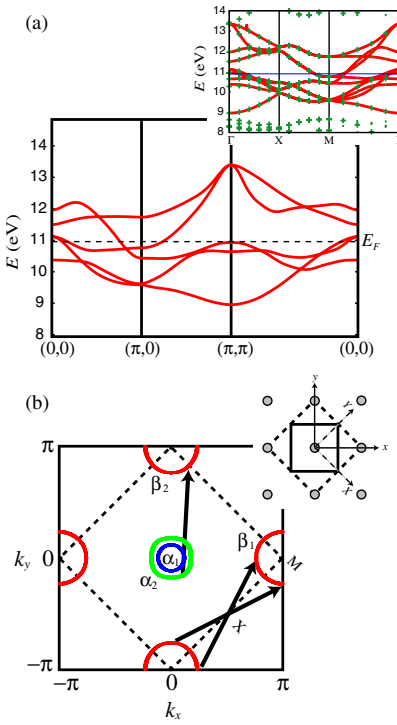

FIG. 1 (color online). (a) The band structure of the five-band model in the unfolded BZ, where the interlayer hoppings are included. To compare with the ten-band model (thick red lines in the inset; the symbols are the present local-density approximation results), note the original (dashed lines) and the unfolded (solid lines) BZ shown in (b). (b) Fermi surface for $n = 6.1$ (with the interlayer hoppings ignored), with the arrows indicating the nesting vectors. Inset depicts the original (dashed lines) and reduced (solid lines) unit cell in real space.

one orbital per symmetry by unfolding the Brillouin zone (BZ) [21], and we end up with an effective five-band model on a square lattice, where x and y axes are rotated by 45° from X-Y [Fig. 1(b), inset], to which we refer for all the wave vectors hereafter. The in-plain hopping integrals $t(\Delta x, \Delta y, \Delta z = 0; \mu, \nu)$ are displayed in Table I, where $[\Delta x, \Delta y]$ is the hopping vector, and μ, ν label the five Wannier orbitals. The on-site energies for the five orbitals are $(\varepsilon_1, \varepsilon_2, \varepsilon_3, \varepsilon_4, \varepsilon_5) = (10.75, 10.96, 10.96, 11.12, 10.62)$ eV. With these effective hoppings and on-site energies, the in-plane tight-binding Hamiltonian is given in the form

$$H_0 = \sum_{ij}\sum_{\mu\nu}\sum_{\sigma}[t(x_i - x_j, y_i - y_j; \mu, \nu)c^{\dagger}_{i\mu\sigma}c_{j\nu\sigma} + t(x_j - x_i, y_j - y_i; \nu, \mu)c^{\dagger}_{j\nu\sigma}c_{i\mu\sigma}] + \sum_{i\mu\sigma}\varepsilon_{\mu}n_{i\mu\sigma}, \quad (1)$$

where $c^{\dagger}_{i\mu\sigma}$ creates an electron with spin σ on the μth orbital at site i, and $n_{i\mu\sigma} = c^{\dagger}_{i\mu\sigma}c_{i\mu\sigma}$. We define the band filling n as the number of electrons per number of sites (e.g., $n = 10$ for full filling). The doping level x in $LaFeAsO_{1-x}F_x$ is related to the band filling as $n = 6 + x$.

In the obtained band structure in Fig. 1(a), we notice that the five bands are heavily entangled, reflecting strong hybridization (see Table I) of the five $3d$ orbitals, which is physically due to the tetrahedral coordination of As atoms around Fe. Hence we conclude that the minimal electronic model requires all five bands. In Fig. 1(b), the Fermi surface for $n = 6.1$ (corresponding to $x = 0.1$) obtained by ignoring the interlayer hoppings is shown in the 2D unfolded BZ. The Fermi surface consists of four pieces (pockets in two dimensions): two concentric hole pockets (denoted as α_1, α_2) centered around $(k_x, k_y) = (0, 0)$, two electron pockets around $(\pi, 0)$ (β_1) or $(0, \pi)$ (β_2), respectively. α_i (β_i) corresponds to the Fermi surface around the ΓZ (MA) line (in the original BZ) in the first-principles band calculation [14,16,17].

Having constructed the model, we now move on to the RPA calculation. We again adopt the 2D model in which the interlayer hoppings are neglected [22]. For the many-body part of the Hamiltonian, we consider the standard interaction terms that comprise the intraorbital Coulomb U, the interorbital Coulomb U', the Hund coupling J, and the pair-hopping J'. All calculations are done in the orbital representation. Details of the multiorbital RPA calculation can be found in, e.g., Refs. [23,24]. The modification of the band structure due to the self-energy correction is not taken into account, on which we comment later. In the present case, the Green function is a 5×5 matrix, while the spin and the orbital susceptibilities become 25×25 matrices. The Green function and the effective pairing interactions, obtained from the susceptibilities, are plugged into the linearized Eliashberg equation, and the gap function in a 5×5 matrix form along with the eigenvalue λ is obtained. T_c corresponds to the temperature where λ reaches unity. 32×32 k-point meshes and 1024 Matsubara frequencies are taken. We find that the spin fluctuations dominate over orbital fluctuations as far as $U > U'$, so we focus on the spin susceptibility. We denote the largest eigenvalue of the spin susceptibility matrix for $i\omega_n = 0$ as $\chi_s(\boldsymbol{k})$. The gap function matrix at the lowest Matsubara frequency is transformed into the band representation by a unitary transformation, and its diagonal element for band i is denoted as $\phi_i(\boldsymbol{k})$.

Let us first look at the result for χ_s for $U = 1.2$, $U' = 0.9$, $J = J' = 0.15$, and $T = 0.02$ (all in units of eV) in Fig. 2(a). The spin susceptibility has peaks around $(k_x, k_y) = (\pi, 0), (0, \pi)$ and also a ridgelike structure from $(\pi, \pi/2)$ to $(\pi/2, \pi)$. This in fact reflects the Fermi surface in Fig. 1(b), where we have two kinds of nesting vector: $\sim(\pi, 0), (0, \pi)$ across α and β, and $\sim(\pi, \pi/2), (\pi/2, \pi)$ across β_1 and β_2. Good nesting enhances tendency towards magnetism. In the RPA (where the self-energy correction in the Green function is neglected), we have to take U as small as 1.2 eV to ensure magnetic ordering does not take place in the temperature range considered.

For SC, we show in Figs. 2(c) and 2(d) the gap function for bands 3 and 4 (as counted from below), together with

TABLE I. Hopping integrals $t(\Delta x, \Delta y; \mu, \nu)$ in units of 0.1 eV. $[\Delta x, \Delta y]$ denotes the in-plain hopping vector, and (μ, ν) the orbitals. σ_y, I, and σ_d correspond to $t(\Delta x, -\Delta y; \mu, \nu)$, $t(-\Delta x, -\Delta y; \mu, \nu)$, and $t(\Delta y, \Delta x; \mu, \nu)$, respectively, where "$\pm$"and "$\pm(\mu', \nu')$" in the (μ, ν) row mean that the corresponding hopping is equal to $\pm t(\Delta x, \Delta y; \mu, \nu)$ and $\pm t(\Delta x, \Delta y; \mu', \nu')$, respectively. This table, combined with the relation $t(\Delta x, \Delta y; \mu, \nu) = t(-\Delta x, -\Delta y; \nu, \mu)$, gives all the in-plain hoppings ≥ 0.01 eV up to fifth neighbors.

$[\Delta x,\Delta y]$ / $[\mu,\nu]$	[1, 0]	[1, 1]	[2, 0]	[2, 1]	[2, 2]	σ_y	I	σ_d
(1, 1)	−0.7		−0.4	0.2	−0.1	+	+	+
(1, 2)	−0.8					−(1, 3)	−	−
(1, 3)	0.8	−1.5			−0.3	−(1, 2)	−	+
(1, 4)		1.7			−0.1	−	+	+
(1, 5)	−3.0			−0.2		+	+	−
(2, 2)	−2.1	1.5				+(3, 3)	+	+
(2, 3)	1.3		0.2	−0.2		+	+	−
(2, 4)	1.7			0.2		+(3, 4)	−	−
(2, 5)	−2.5	1.4				−(3, 5)	−	+
(3, 3)	−2.1	3.3		−0.3	0.7	+(2, 2)	+	+
(3, 4)	1.7	0.2		0.2		+(2, 4)	−	+
(3, 5)	2.5			0.3		−(2, 5)	−	−
(4, 4)	1.6	1.2	−0.3	−0.3	−0.3	+	+	+
(4, 5)				−0.1		−	+	−
(5, 5)	3.1	−0.7	−0.2			+	+	+

the Fermi surface of each band. At this temperature ($T = 0.02$), the eigenvalue of the Eliashberg equation is $\lambda = 0.96$ [25]. The gap is basically an s wave, but changes sign between the Fermi surface of band 3 (α_2) (and also band 2; α_1 not shown) and those of band 4 (β_1, β_2), namely, across the nesting vector $\sim(\pi, 0)$, $(0, \pi)$ (M point in the original BZ) at which the spin fluctuations develop. Such a sign change of the gap between inner hole and outer electron Fermi pockets is analogous to those in models studied by Bulut *et al.* [26], and also by two of the present authors [27,28]. It is also reminiscent of the unconventional s-wave pairing mechanism for $Na_xCoO_2 \cdot yH_2O$ [29] proposed by four of the present authors [30]. After completion of the present study, we have come to notice that a recent study by Mazin *et al.* also concludes an s-wave pairing in which the gap changes sign between α and β Fermi surfaces [31], as schematically shown in the upper panel of Fig. 2(b). For the present set of parameter values, in addition to this sign change, we find that the nodes of the gap intersect the β Fermi surface. This is because the spin fluctuations due to the β_1-β_2 nesting favor a sign change in the gap between β_1 and β_2 Fermi surfaces. In fact, we have found that this nodal line moves out of the β Fermi surface for the parameter values for which the spin fluctuations due to the β_1-β_2 nesting become less effective, e.g., for $U = U'$. In that case, the gap becomes closer to the upper panel of Fig. 2(b) [32].

We have so far focused on the diagonal elements of the gap matrix in the band representation, but to be more precise, we have to consider the off-diagonal (interband) elements in order to make an accurate comparison with the experiments. The off-diagonal elements in the present case turn out to be not negligibly small due to the heavy entanglement of the bands. One way to look at this effect is to calculate the quantity $\sqrt{(\hat{\phi}\hat{\phi}^\dagger)_{44}}$, where $\hat{\phi}$ is the gap matrix and 44 denotes the diagonal element of band 4. As shown in Fig. 2(e), we find that this quantity is finite over the entire BZ, but a remnant of the nodal lines of the diagonal element still appears as a valley that intersects the β Fermi surface. In this sense, we can say that the magnitude of the gap varies along the β Fermi surface (becomes large at points far from the BZ edge) if the spin fluctuations arising from α-β and β_1-β_2 interactions have competing strength. The degree of the variation of the gap in the actual materials may be determined experimentally from the density of states, e.g., tunneling spectroscopy, or directly by angle resolved photoemission studies.

In the above, we mainly considered the possibility of unconventional s-wave pairing. On the other hand, if the α Fermi surfaces are absent (or less effective), the simplest form of the gap would be the $d_{x^2-y^2}$-wave pairing (d_{XY} in the original BZ), where the gap changes sign between β_1 and β_2 Fermi surfaces as shown in the lower panel of Fig. 2 (b). To check this, we have performed an RPA calculation on (i) the present model with $n = 6.3$ and (ii) a model where we artificially shift the crystal field splitting to let the α Fermi surfaces disappear for $n = 6.1$. In both cases, we indeed obtain the $d_{x^2-y^2}$ wave. Since the band structure generally changes from the local-density approximation result due to correlation effects [16] or a band filling different from the formally expected value, we leave, at the present stage, this d-wave state as another candidate for the pairing symmetry in this material.

Many other interesting problems remain for future studies. Spin fluctuations and SC should be studied by taking

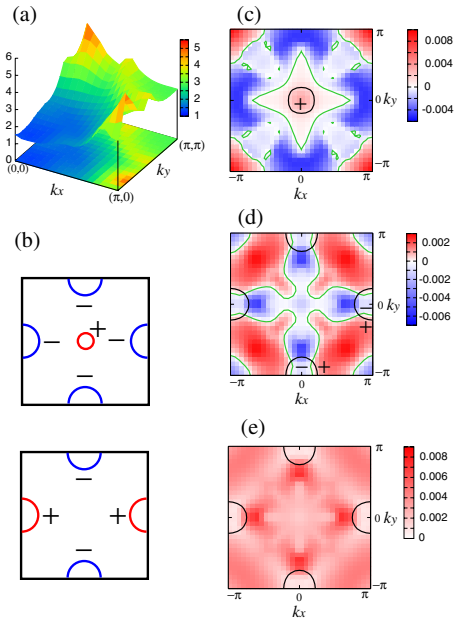

FIG. 2 (color online). RPA result for the spin susceptibility χ_s (a), the gap functions ϕ_3 (c) and ϕ_4 (d), $\sqrt{(\hat{\phi}\hat{\phi}^\dagger)_{44}}$ (e) for $U = 1.2$, $U' = 0.9$, $J = J' = 0.15$, $n = 6.1$, and $T = 0.02$ (in eV). In (c) and (d), the black (green or light gray) solid lines represent the Fermi surfaces (gap nodes). In (b), the fully gapped extended s-wave (upper panel) and $d_{x^2-y^2}$-wave gaps are schematically shown.

into account the self-energy correction, for which a fluctuation exchange [33] study is underway [34]. It is also intriguing to investigate whether the present unconventional gap can quantitatively account for the specific-heat [7] and point-contact conductance [8] results. Also, further insight into the origin of the high T_c SC in $LaFeAsO_{1-x}F_x$ may be obtained by performing similar microscopic studies on $LaFePO_{1-x}F_x$ [4] or LaNiPO [5].

We are grateful to Hideo Hosono for fruitful discussions and providing us with the lattice structure data prior to publication. R. A. is grateful to Kazuma Nakamura for discussions on the Wannier orbitals. Numerical calculations were performed at the facilities of the Information Technology Center, University of Tokyo, and also at the Supercomputer Center, ISSP, University of Tokyo. This study has been supported by Grants-in-Aid for Scientific Research from MEXT of Japan and from the Japan Society for the Promotion of Science.

*Present Address: Department of Applied Physics, University of Tokyo, Hongo, Tokyo 113-8656, Japan.

[1] Y. Kamihara *et al.*, J. Am. Chem. Soc. **130**, 3296 (2008).
[2] B. I. Zimmer *et al.*, J. Alloys Compd. **229**, 238 (1995).
[3] P. Quebe *et al.*, J. Alloys Compd. **302**, 70 (2000).
[4] Y. Kamihara *et al.*, J. Am. Chem. Soc. **128**, 10 012 (2006).
[5] T. Watanabe *et al.*, Inorg. Chem. **46**, 7719 (2007).
[6] G. F. Chen *et al.*, arXiv:0803.0128 [Phys. Rev. Lett. (to be published)].
[7] G. Mu *et al.*, Chin. Phys. Lett. **25**, 2221 (2008).
[8] L. Shan *et al.*, arXiv:0803.2405.
[9] C.-R. Hu, Phys. Rev. Lett. **72**, 1526 (1994).
[10] Y. Tanaka and S. Kashiwaya, Phys. Rev. Lett. **74**, 3451 (1995).
[11] S. Kashiwaya and Y. Tanaka, Rep. Prog. Phys. **63**, 1641 (2000).
[12] T. Löfwander *et al.*, Supercond. Sci. Technol. **14**, R53 (2001).
[13] X. Zhu *et al.*, Supercond. Sci. Technol. **21**, 105001 (2008).
[14] S. Lebégue, Phys. Rev. B **75**, 035110 (2007).
[15] D. J. Singh and M.-H. Du, Phys. Rev. Lett. **100**, 237003 (2008).
[16] K. Haule *et al.*, Phys. Rev. Lett. **100**, 226402 (2008).
[17] G. Xu *et al.*, Europhys. Lett. **82**, 67 002 (2008).
[18] L. Boeri *et al.*, Phys. Rev. Lett. **101**, 026403 (2008).
[19] S. Baroni *et al.*, http://www.pwscf.org/. Here we adopt the exchange correlation functional introduced by J. P. Perdew *et al.* [Phys. Rev. B **54**, 16 533 (1996)], and the wave functions are expanded by plane waves up to a cutoff energy of 40 Ry. Also, 10^3 k-point meshes are used with the special points technique by H. J. Monkhorst and J. D. Pack [Phys. Rev. B **13**, 5188 (1976)].
[20] N. Marzari and D. Vanderbilt, Phys. Rev. B **56**, 12 847 (1997); I. Souza *et al.*, Phys. Rev. B **65**, 035109 (2001). The Wannier functions are generated by the code developed by A. A. Mostofi *et al.* (http://www.wannier.org/) for the energy window $-2\ \text{eV} < \epsilon_k - E_F < 2.6\ \text{eV}$ is the eigenenergy of the Bloch states and E_F the Fermi energy.
[21] While an ambiguity exists in unfolding the BZ [if the sign of the hoppings $t(\Delta x, \Delta y; \mu, \nu)$ with $\Delta x + \Delta y =$ odd (i.e., hoppings between A and B sites in a bipartite lattice) is changed, a band structure is reflected with respect to $|k_x| + |k_y| = \pi$], this is just a unitary transformation, and either way the five-band structure gives the same ten bands in the folded BZ as well as the same RPA results.
[22] Quasi-2D systems are generally more favorable than 3D for spin-fluctuation mediated SC as shown by P. Monthoux and G. G. Lonzarich, Phys. Rev. B **59**, 14 598 (1999); R. Arita *et al.*, *ibid.* **60**, 14 585 (1999).
[23] K. Yada and H. Kontani, J. Phys. Soc. Jpn. **74**, 2161 (2005).
[24] T. Takimoto *et al.*, Phys. Rev. B **69**, 104504 (2004).
[25] The λ value should be reduced if the self-energy corrections are considered as in the fluctuation exchange method.
[26] N. Bulut *et al.*, Phys. Rev. B **45**, 5577 (1992).
[27] K. Kuroki and R. Arita, Phys. Rev. B **64**, 024501 (2001).
[28] K. Kuroki *et al.*, Phys. Rev. B **66**, 184508 (2002).
[29] K. Takada, Nature (London) **422**, 53 (2003).
[30] K. Kuroki *et al.*, Phys. Rev. B **73**, 184503 (2006).
[31] I. I. Mazin *et al.*, arXiv:0803.2740 [Phys. Rev. Lett. (to be published)].
[32] The situation is reminiscent of a 3D case of disconnected Fermi surface studied in S. Onari *et al.*, Phys. Rev. B **65**, 184525 (2002), where the presence of intra- and interpocket nestings dominates the pairing symmetry.
[33] N. E. Bickers *et al.*, Phys. Rev. Lett. **62**, 961 (1989).
[34] S. Onari *et al.* (to be published).